J. Engg. Math., 16, 171–180 (1982). 0022–0833/82/02/0171–10 $00.20/0

Non-linear, drag-free flow over a submerged semi-elliptical body

L. K. FORBES

*Department of Applied Mathematics, University of Adelaide, Adelaide, Australia**

(Received June 2, 1981)

SUMMARY

Two-dimensional steady flow of an ideal fluid with a free surface over a semi-elliptical body attached to the bottom of a stream is considered. A numerical method is presented for computing the values of the ellipse length at which the non-linear wave train normally present downstream of the body vanishes, and the semi-elliptical body therefore experiences no wave resistance. These special ellipse lengths are shown to be such strong functions of the ellipse height that the predictions of linearized theory are grossly inadequate in general.

Introduction

In a recent paper of the author [1], the two-dimensional free-surface flow of an ideal fluid over a semi-elliptical bump on the bottom of a running stream was investigated. The free surface was shown to possess a local disturbance above the semi-elliptical body, followed in general by a train of non-linear downstream waves. The energy radiated away to infinity by this wave train is balanced by a horizontal force component (the wave resistance) acting on the body.

A linearized solution to this problem was developed by Lamb [2, p. 409]. A feature of Lamb's theory is that the downstream wave train is predicted to vanish for ellipses of certain special lengths, resulting in a wave resistance of precisely zero in these instances. In fact, there is a countably infinite set of ellipse lengths for which the wave drag vanishes, when the ellipse height and the upstream Froude number of the flow are both fixed.

It was demonstrated in our previous paper [1] that solutions possessing no downstream wave train are also obtained in the fully non-linear problem, and, as with the linearized theory of Lamb, there is probably an infinite spectrum of ellipse lengths for which such solutions occur, for fixed upstream Froude number and ellipse height. However, unlike Lamb's theory, these special ellipse lengths are also strong functions of the ellipse height, as well as of the upstream Froude number. These findings are consistent with recent work of von Kerczek and Salvesen [3] and Schwartz [4], who considered the effects of a given pressure distribution applied to the surface of a running stream.

In this paper, we present a numerical method for explicitly determining those values of the

*Current address: Institute of Hydraulic Research, University of Iowa, Iowa City, Iowa 52242, U.S.A.

ellipse length at which the non-linear wave drag vanishes. The problem is formulated as in Forbes [1], by first transforming the bottom into a straight line, and then seeking the solution in the inverse plane, with the velocity potential and streamfunction as the independent variables. The free-surface profile and the ellipse length are obtained using an efficient boundary-integral formulation of the problem, which involves values of the unknown functions over only half of the free surface; consequently, there is no need to place numerical grid points throughout the entire fluid region. The results are expected to be of importance in the design of certain underwater craft.

2. Formulation of the problem

Consider a semi-ellipse of length $2R_X$ and height R_Y placed on the bottom of a running stream, with the origin of a cartesian coordinate system at the centre of the ellipse, and the y-axis pointing vertically. The fluid is incompressible and flows without rotation. Far upstream the flow is uniform, with depth H and speed c. The fluid is subject to the downward acceleration of gravity, g.

The problem is immediately non-dimensionalized, by referring all lengths to the quantity H, the horizontal and vertical components of velocity (u and v) to the speed c, and the velocity potential ϕ and streamfunction ψ to the product cH. Thus the bottom is the streamline $\psi = 0$ and the surface is $\psi = 1$. The three dimensionless parameters of the flow are

$$F = \frac{c}{(gH)^{1/2}}, \qquad \alpha = \frac{R_X}{H} \qquad \text{and} \qquad \beta = \frac{R_Y}{H},$$

where F is the upstream Froude number, and α and β are the dimensionless ellipse half-length and height, respectively. The non-dimensional flow situation is depicted in Figure 1.

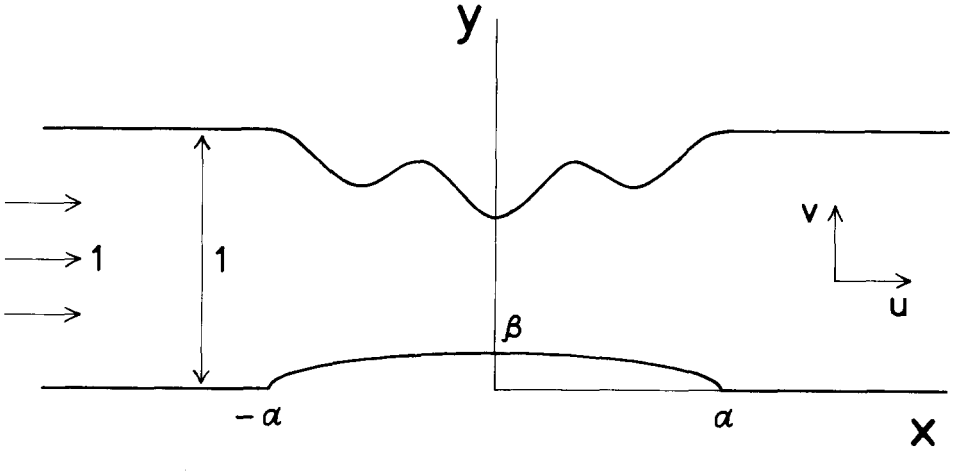

Figure 1. The non-dimensional flow situation in the z-plane.

At the free surface of the fluid, we impose the Bernoulli equation

$$\tfrac{1}{2}F^2(u^2+v^2)+y = \tfrac{1}{2}F^2+1. \tag{1}$$

The condition of no flow normal to the bottom $y = h(x)$ is expressed by the equation

$$u\frac{dh}{dx} = v \quad \text{on} \quad y = h(x) \tag{2}$$

where

$$h(x) = \begin{cases} 0 & , \ |x| \geqslant \alpha \\ \dfrac{\beta}{\alpha}(\alpha^2 - x^2)^{1/2}, & |x| \leqslant \alpha. \end{cases}$$

Since the fluid is incompressible and flows irrotationally, it follows that the complex potential $f = \phi + i\psi$ may be expressed as an analytic function of $z = x + iy$. In order to correctly account for the fluid behaviour at the stagnation points at $z = \pm\alpha$, the channel bed is transformed into a straight line, by means of the conformal map

$$z = \tau + \frac{\beta}{\alpha}(\tau^2 - \alpha^2)^{1/2}, \tag{3}$$

where the new variable is written $\tau = \xi + i\eta$. Following Forbes [1], the rôles of the variables f and τ are now interchanged, so that the quantity $\tau = \xi + i\eta$ is to be sought as an analytic function of the independent variable $f = \phi + i\psi$. In the f-plane, the Bernoulli equation (1) becomes

$$\tfrac{1}{2}F^2 \frac{\alpha^2(A^2+B^2)}{(\alpha A+\beta\xi)^2+(\alpha B+\beta\eta)^2} \frac{1}{\tau_\phi\bar{\tau}_\phi} + \eta + \frac{\beta}{\alpha}B = \tfrac{1}{2}F^2 + 1 \quad \text{on} \quad \psi = 1, \tag{4}$$

where we have defined

$$(\tau^2 - \alpha^2)^{1/2} = A + iB.$$

The bar and the subscripts denote complex conjugation and partial differentiation, respectively. The bottom condition (2) now takes the simple form

$$\eta = 0 \quad \text{on} \quad \psi = 0. \tag{5}$$

In reference [1] it was shown that the real and imaginary parts of the function $d\tau/df$ at the free surface $\psi = 1$ are related by means of the integro-differential equation

$$\left[\xi_\phi(\phi,1)-\left(1+\frac{\beta}{\alpha}\right)^{-1}\right]-\frac{2}{\pi}\int_{-\infty}^{\infty}\left[\xi_\theta(\theta,1)-\left(1+\frac{\beta}{\alpha}\right)^{-1}\right]\frac{d\theta}{(\theta-\phi)^2+4}$$

$$=-\frac{1}{\pi}\left\{\int_{-\infty}^{\infty}\frac{\eta_\theta(\theta,1)d\theta}{\theta-\phi}+\int_{-\infty}^{\infty}\frac{\eta_\theta(\theta,1)(\theta-\phi)d\theta}{(\theta-\phi)^2+4}\right\}. \tag{6}$$

Note that the bottom condition (5) has been satisfied automatically in equation (6), by reflection about $\psi = 0$.

In the present problem, we seek the special values of the ellipse half-length α for which the wave drag is zero. There is thus no downstream wave train, and consequently, the surface profile is symmetric about $\phi = 0$ ($\xi = 0$). Equation (6) may therefore be written

$$\left[\xi_\phi(\phi,1)-\left(1+\frac{\beta}{\alpha}\right)^{-1}\right]$$

$$-\frac{2}{\pi}\int_0^{\infty}\left[\xi_\theta(\theta,1)-\left(1+\frac{\beta}{\alpha}\right)^{-1}\right]\left[\frac{1}{(\theta-\phi)^2+4}+\frac{1}{(\theta+\phi)^2+4}\right]d\theta$$

$$=-\frac{1}{\pi}\int_0^{\infty}\eta_\theta(\theta,1)\left[\frac{1}{\theta-\phi}+\frac{1}{\theta+\phi}\right]d\theta$$

$$-\frac{1}{\pi}\int_0^{\infty}\eta_\theta(\theta,1)\left[\frac{(\theta-\phi)}{(\theta-\phi)^2+4}+\frac{(\theta+\phi)}{(\theta+\phi)^2+4}\right]d\theta. \tag{7}$$

The solution is thus obtained by solving equation (7) coupled with the Bernoulli equation (4), and subject to the condition

$$z \to f \quad \text{as} \quad \phi \to \pm\infty, \tag{8}$$

which is necessary to prevent a wave train from appearing either upstream or downstream of the ellipse. The solution is obtained parametrically, in the form $(\xi(\phi,1), \eta(\phi,1))$, and the original variables x and y are recovered from equation (3). The problem thus posed is, in fact, a non-linear eigenvalue problem, in which the eigenvalue is the ellipse half-length α, and the shape of the free surface is the associated eigenfunction.

3. Numerical methods

The numerical method for the solution of the system of equations (4), (7) and (8) is similar to that described in previous papers [1, 4, 5], and consists of attempting to satisfy the equations

at $N+1$ equally spaced free-surface points $\phi_0, \phi_1, \ldots, \phi_N$. Here, $\phi_0 = 0$, and ϕ_N is chosen to be an appropriately large, positive number.

The integrals in equation (7) are first truncated downstream at the point ϕ_N, and the equation is evaluated at the N midpoints $\phi_{k-1/2}, k = 1, 2, \ldots, N$. The singularity is subtracted from the Cauchy Principal Value integral, and the integrals are discretized using Simpson's Rule. A three-point interpolation formula, consistent with the parabolae fitted by Simpson's Rule, is used to express the quantities ξ_ϕ and η_ϕ at the midpoints in terms of values of these quantities at the mesh points ϕ_j, $j = 0, 1, \ldots, N$. Thus equation (7) is replaced by a matrix system of the form

$$\sum_{j=1}^{N} a_{kj}\left[\xi'_j - \left(1+\frac{\beta}{\alpha}\right)^{-1}\right] = \sum_{j=1}^{N-1} b_{kj}\eta'_j + c_k\left[\xi'_0 - \left(1+\frac{\beta}{\alpha}\right)^{-1}\right] + d_k\eta'_0 + e_k\eta'_N, \quad k = 1, \ldots, N,$$

in which the quantities a_{kj}, b_{kj} etc. are functions only of ϕ and of the integration and interpolation formulae. The primes denote differentiation. Upon inversion of a matrix, the solution is obtained in the form

$$\xi'_i = \left(1+\frac{\beta}{\alpha}\right)^{-1} + \sum_{j=1}^{N-1} H_{ij}\eta'_j + H_{iN}\left[\xi'_0 - \left(1+\frac{\beta}{\alpha}\right)^{-1}\right] + H_{iN+1}\eta'_0 + H_{iN+2}\eta'_N, \quad i = 1, \ldots, N. \tag{9}$$

The symmetry of the surface profile about $\phi_0 = 0$ results in the conditions

$$\xi_0 = \eta'_0 = 0. \tag{10}$$

In order to satisfy equation (8), we impose the following approximate conditions at the last point ϕ_N downstream:

$$\eta_N = \frac{\alpha}{\alpha^2-\beta^2}\{\alpha - \beta \operatorname{Im}[(\phi_N + i)^2 - \alpha^2 + \beta^2]^{1/2}\}, \qquad \eta'_N = 0. \tag{11}$$

The trapezoidal rule is now used to obtain η at the remaining free-surface points. Thus

$$\eta_i = \eta_N - h(\tfrac{1}{2}\eta'_N + \eta'_{N-1} + \ldots + \eta'_{i+1} + \tfrac{1}{2}\eta'_i), \qquad i = N-1, \ldots, 1, 0, \tag{12}$$

where h denotes the spacing between mesh points and is defined as $h = (\phi_N - \phi_0)/N$. The Bernoulli equation at the first point ϕ_0 enables the quantity ξ'_0 to be eliminated in favour of quantities at the remaining free-surface points, according to the formula

$$\xi_0' = \frac{1}{2} F \frac{\alpha B_0}{\alpha B_0 + \beta \eta_0} \left[\frac{2}{\frac{1}{2} F^2 + 1 - \eta_0 - \frac{\beta}{\alpha} B_0} \right]^{1/2}, \tag{13}$$

where the variable B is defined in equation (4). Finally, the function ξ is obtained from the trapezoidal rule

$$\xi_i = \xi_0 + h(\tfrac{1}{2}\xi_0' + \xi_1' + \ldots + \xi_{i-1}' + \tfrac{1}{2}\xi_i'), \quad i = 1, 2, \ldots, N. \tag{14}$$

The Bernoulli equation (4), evaluated at the points ϕ_j, $j = 1, \ldots, N$, yields a system of N algebraic equations in the N unknowns η_1', $\eta_2', \ldots, \eta_{N-1}'$, α, after all other quantities have been eliminated using equations (9)–(14). This system may be written

$$P_i(\eta_1', \eta_2', \ldots, \eta_{N-1}', \alpha) = 0, \quad i = 1, \ldots, N, \tag{15}$$

where P_i denotes the pressure at the i-th free-surface point.

Equations (15) are solved by a Newtonian iteration scheme. Thus the solution at the k-th iteration is updated for the $(k+1)$ — st iteration according to the formulae

$$\begin{aligned} \eta_i'^{(k+1)} &= \eta_i'^{(k)} + \Delta_i, \quad i = 1, \ldots, N-1 \\ \alpha^{(k+1)} &= \alpha^{(k)} + \Delta_N, \end{aligned} \tag{16}$$

where the vector Δ is the solution to the matrix equation

$$\begin{bmatrix} \frac{\partial P_1^{(k)}}{\partial \eta_1'} & \cdots & \frac{\partial P_1^{(k)}}{\partial \eta_{N-1}'} & \frac{\partial P_1^{(k)}}{\partial \alpha} \\ \vdots & & \vdots & \vdots \\ \frac{\partial P_N^{(k)}}{\partial \eta_1'} & \cdots & \frac{\partial P_N^{(k)}}{\partial \eta_{N-1}'} & \frac{\partial P_N^{(k)}}{\partial \alpha} \end{bmatrix} \begin{bmatrix} \Delta_1 \\ \vdots \\ \Delta_N \end{bmatrix} = - \begin{bmatrix} P_1^{(k)} \\ \vdots \\ P_N^{(k)} \end{bmatrix} \tag{17}$$

The derivatives in the Jacobian matrix in equation (17) were approximated by forward differences. If the root-mean-squared residual pressure, P_{rms}, is greater at the $(k+1)$ — st iteration than at the k-th, then the vector Δ is halved and the iteration (16) is repeated.

The numerical solution of the non-linear eigenvalue problem defined by equations (4), (7) and (8) therefore proceeds as follows: firstly, an initial guess is made for the unknowns $\eta_1', \ldots, \eta_{N-1}'$, α. An approximation based on Lamb's linearized solution (see [1, eq. 14]) is usually sufficient for this purpose. Thus we take

$$\eta'(\phi, 1) = -\beta \int_0^\infty \frac{\kappa J_1(\alpha_s \kappa) \sin(\kappa \phi)}{\kappa \cosh(\kappa) - \frac{1}{F^2} \sinh(\kappa)} \, d\kappa \tag{18}$$

with

$$\alpha_s = \frac{j_{1,s}}{\kappa_0}, \quad s = 1, 2, \ldots,$$

where κ_0 is the positive real root of the transcendental equation

$$\tanh(\kappa_0) = F^2 \kappa_0.$$

The function J_1 is the first kind Bessel function of order one, and $j_{1,s}$ are its zeros. The non-linear eigensolution desired is usually obtained from the Newtonian iterations simply by choosing the appropriate value of s in the initial guess (18). Secondly, the pressure is computed at each free-surface point using equations (9)–(15). If $P_{\text{rms}} < 10^{-10}$, the Newtonian process is stopped. Thirdly, a new estimate for the unknowns is obtained from equations (16) and (17). The process is now returned to the second step.

Solutions to equations (15) are usually obtained rapidly, due to the quadratic convergence of Newton's method. When $N = 130$, a converged non-linear free-surface profile is obtained from the initial guess (18) in about four iterations. The error involved in the discretization of the exact equations is nominally of the order of the cube of the spacing h between free-surface points; consequently, truncation error in the present problem is extremely small.

4. Discussion of results

In Figure 2, three non-linear free-surface profiles are shown for the case $F = 0.8$, $\beta = 0.02$, for the first three values of the ellipse half-length α at which the non-linear wave resistance vanishes. These profiles are symmetric about the centre-line $x = 0$. As in previous work [1, 5], it is found that a spurious wave train of extremely small amplitude is present downstream. It is a simple matter to demonstrate that this wave train is numerically generated and has no physical significance; in fact, it is a consequence of the truncation of the integro-differential equation (7) downstream at the last point ϕ_N, and the subsequent imposition of the approximate conditions (11) there.

The values of α at which the first two eigensolutions occur are $\alpha_1 = 3.973$ and $\alpha_2 = 6.660$, where α_s denotes the value of α at which the s-th non-linear eigensolution occurs. These results are in excellent agreement with the previous estimates $\alpha_1 \sim 3.95$, $\alpha_2 \sim 6.6$ given by Forbes [1] for the same values of F and β. Note that for the second eigensolution, there is a single 'trapped wave' in the portion of the fluid above the semi-elliptical body, although no waves are present in the far field. For the third eigensolution, two 'trapped waves' are present above the body. In general, it appears that the s-th eigensolution possesses $s - 1$ waves 'trapped' in the region above the semi-ellipse.

In the linearized theory of Lamb, the values of the ellipse half-length α_s, $s = 1, 2, \ldots$ at which drag-free solutions exist are functions only of F, and are independent of the ellipse height β. However, in the fully non-linear problem, the eigenvalues α_s are also strong functions of β. This is illustrated in Figure 3 for the first four eigensolutions, when the upstream Froude number is $F = 0.5$. The predictions of Lamb's theory, computed from equation (18) with

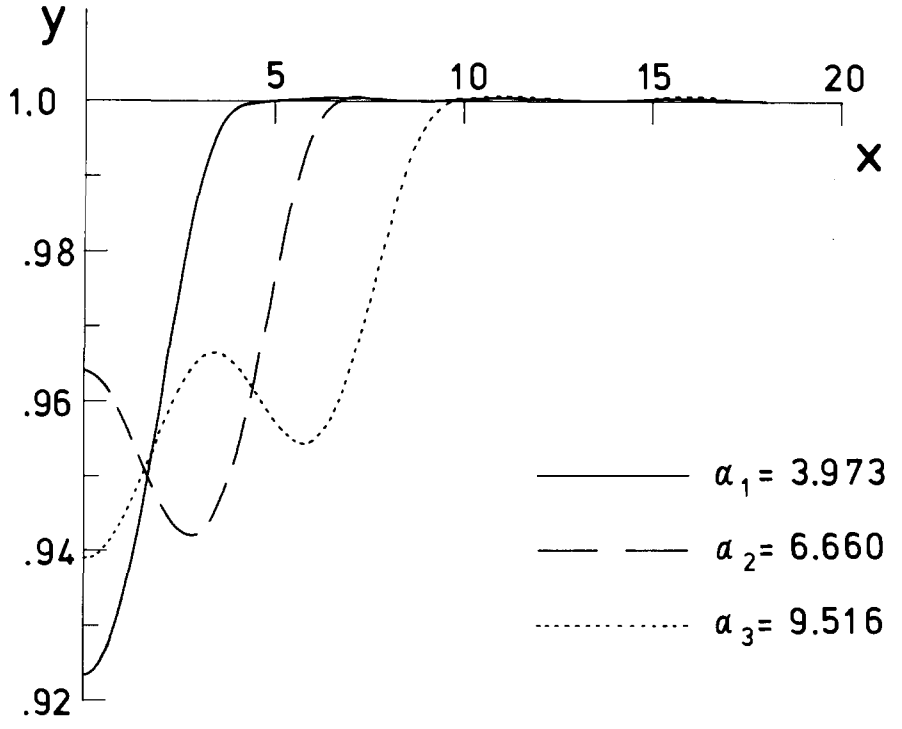

Figure 2. Three non-linear free-surface profiles for the case $F = 0.8$, $\beta = 0.02$, obtained for the first three eigensolutions.

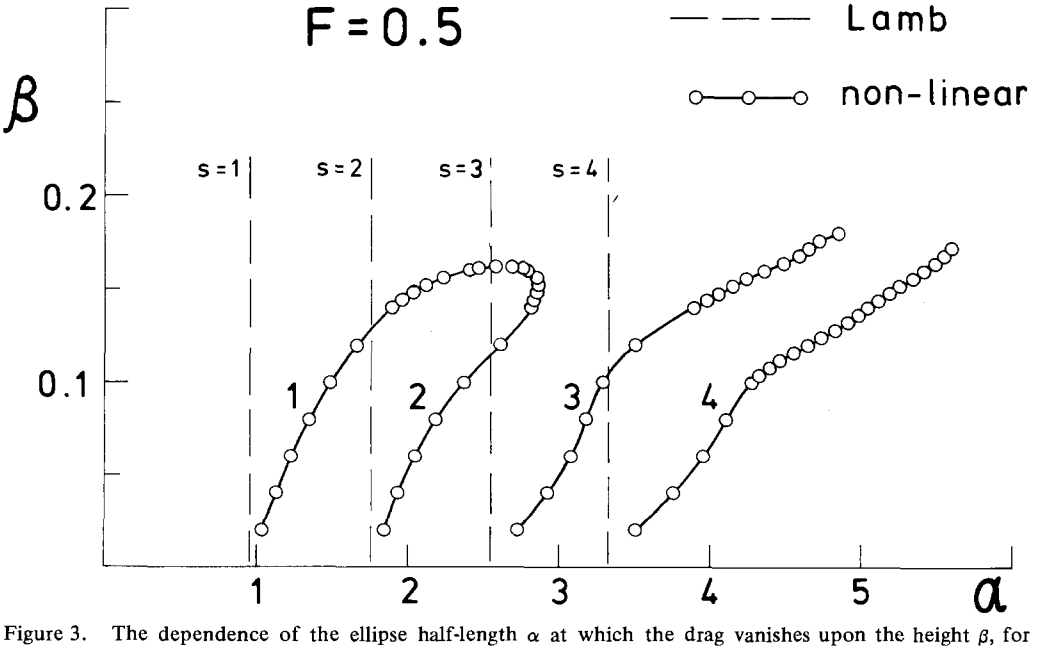

Figure 3. The dependence of the ellipse half-length α at which the drag vanishes upon the height β, for $F = 0.5$. Results obtained from the linearized and non-linear problems are shown, for the first four eigensolutions.

$s = 1, \ldots, 4$, are indicated with dashed lines on the diagram; since there is no dependence of α_s upon β in this theory, a series of vertical lines at the values of α given by equation (18) are obtained. The open circles in Figure 3 represent results obtained from 68 converged non-linear free-surface profiles, for the first four non-linear eigensolutions, numbered 1 to 4 respectively on the diagram. The various non-linear families of solution were traced using a 'bootstrapping' process; a non-linear solution was obtained from the initial guess (18) for a suitably small value of β, and was then used as the initial guess for a problem with β slightly increased, and so on.

It is evident from Figure 3 that the effect of non-linearity upon the eigenvalues α_s is extreme indeed. For small β, the agreement between the linear and non-linear results is reasonably good. (Nevertheless, the linear and non-linear results cannot be expected to agree *exactly* even in the limit $\beta \to 0$, since Lamb's theory does not correctly account for the fluid behaviour at the stagnation points at $z = \pm \alpha$, as described in [5]). However, as β is increased, the values of α_s increase dramatically beyond the predictions of the linearized theory. In the case of the first eigensolution for example, the value of the ellipse half-length α at which a drag-free solution is obtained may become as much as 200% greater than the value of α_1 obtained from linearized theory.

Perhaps the most surprising feature of the non-linear results in Figure 3 is that the first and second eigensolutions ultimately merge together at the limiting value of the ellipse height $\beta \sim 0.162$. For larger values of β, it is apparently not possible to obtain solutions of this type. When β is small, the free surface for solutions of type 2 possesses a single 'trapped wave' in the region above the body, similar to that shown in Figure 2. However, as β is increased, the relative amplitude of this wave decreases, and ultimately vanishes when β is close to the maximum value $\beta \sim 0.162$. Thus there is no doubt that solutions of type 2 evolve continuously into solutions of type 1, and *vice versa*. By contrast, the third and fourth eigensolutions, shown in Figure 3, show no particular tendency to coalesce, and their fate at large β is therefore uncertain. In the case of solutions of type 4, Newton's method was not capable of yielding a converged solution for β larger than the maximum value for this family, $\beta \sim 0.172$, shown on the diagram. For the third eigensolution, results were obtained with β as large as 0.18. Although it appeared that Newton's method would converge for even larger values of β, no attempt was made to seek such solutions, since it appears that results with $\beta \gtrsim 0.17$ are possibly of doubtful accuracy for the third eigensolution.

It has not been possible to determine from our solutions the nature of the physical process responsible for the merging of the first two families of drag-free solutions at $\beta \sim 0.162$. However, it seems reasonable to conjecture that the phenomenon is related to the breaking of the waves formed downstream of the semi-elliptical bump in the general case when the ellipse half-length α takes a value different from the eigenvalues α_s, $s = 1, 2, \ldots$. It is possible that the third and fourth eigensolutions may likewise coalesce for some β.

5. Further remarks

The values of the ellipse length at which the non-linear wave drag on the body vanishes have been shown in the present paper to be extremely strong functions of the ellipse height. For

ellipses of even quite modest height, the linearized theory severely underpredicts the value of the ellipse length at which zero-drag solutions exist.

Since non-linear effects have played such a dominant rôle in the present problem, it is natural to suspect that they may continue to be of equal importance in the practical design of underwater craft, such as submarines, moving beneath a free surface. Of course, the flow about such craft involves additional physical processes, such as circulation about the body and flow of fluid between the body and the bottom, and it is no longer clear that non-linear zero-drag solutions are possible in this case. In addition, it is possible that the effects of non-linearity may be lessened somewhat in the case of fully three-dimensional steady flow about submerged bodies.

6. Acknowledgement:

This work was supported by ARGC (Australian Research Grants Committee) grant number F76/15343R at the University of Adelaide.

References

[1] L. K. Forbes, On the wave resistance of a submerged semi-elliptical body, *J. Eng. Math.* 15 (1981) 287–298.

[2] H. Lamb, *Hydrodynamics*, 6th ed., Cambridge University Press (1932).

[3] C. von Kerczek and N. Salvesen, Nonlinear free-surface effects – the dependence on Froude number, *Proc. 2nd Int. Conf. on Numerical Ship Hydrodynamics* (1977) 292–300.

[4] L. W. Schwartz, Nonlinear solution for an applied overpressure on a moving stream, *J. Eng. Math.* 15 (1981) 147–156.

[5] L. K. Forbes and L. W. Schwartz, Free-surface flow over a semi-circular obstruction, to appear in *J. Fluid Mech.* (1982).